JOURNAL OF COMPUTATIONAL PHYSICS 117, 20–27 (1995)

Dissipation Additions to Flux-Difference Splitting

HONG-CHIA LIN

Department of Mechanical Engineering, Nan-Rong Institute of Technology, Yenshui 73701, Tainan County, Taiwan, Republic of China

Received July 22, 1991; revised October 1994

Although the flux-difference splitting methods for solving the Euler equations are generally very robust and no explicit dissipation is required. There are situations where explicit dissipation is needed. Two cases, a slowly moving shock problem and a blunt body calculation, are discussed in this paper. The slowly moving shock problem is tested extensively by Roe's Riemann solver and a cure for Roe's Riemann solver is proposed. For the second-order scheme it is found necessary to reduce the second-order accuracy to first-order accuracy inside the shock layer. For the supersonic blunt body calculation adding dissipation in the linear waves in Roe's Riemann solver can prevent numerical instability in the subsonic pocket. The drawback of Yee's formula to cure the instability when used on viscous flow calculation is demonstrated. A better solution based on the pressure gradient is proposed.

1. INTRODUCTION

In the past decade there has been tremendous progress in solving the nonlinear hyperbolic system of equations, especially the Euler equations governing inviscid flow problems in fluid dynamics. The flux-difference splitting schemes [1], which employ Riemann solvers, are perhaps the most successful approach in solving such problems. The flux-difference splitting schemes are very robust and usually no explicit dissipation is required; nevertheless there are situations where extra dissipation is needed. Two cases of problems with the Euler equations will be discussed in this paper. The first one is the slowly moving shock problem, which was first discussed by Collela and Woodward [2] and later by Roberts [3]. The second one is the numerical instability, called the "carbuncle phenomenon," associated with blunt body calculation, which was known for some time but only reported recently in literature by Peery and Imlay [4]. This paper differs from previous works by providing more understanding to both problems and possible cures with special emphasis on the Rieman solver of Roe [5].

This paper is organised as follows. In Section 2, we first review the slowly moving shock problem, follow by the numerical result of Roe's Riemann solver. A cure based on explicit dissipation is proposed. A suggestion for second-order schemes is also provided. In Section 3 the carbuncle phenomenon is introduced. The drawback of the popular formula due to Yee [6] when used for Navier–Stokes calculation is demonstrated with a simple boundary layer calculation. An improved solution based on the formula of [4] is demonstrated. Section 4 concludes this paper.

2. THE SLOWLY MOVING SHOCK PROBLEM

2.1 *General Review*

It has been observed for some time that when a shock is moving slowly, some upwind schemes produce wiggles in the post shock region, even when those schemes do not produce oscillations for a scalar equation. This difficulty can only happen in coupled systems, it does not occur in a scalar equation or in systems of equations that can be decoupled.

The non-monotone behaviour is certainly unwanted in unsteady flow calculations. It may also cause convergence difficulty when one uses the time marching approach to find the steady state solution.

The first detailed account of this problem was given by Colella and Woodward [2]. They observed that low amplitude postshock oscillations occurred when the characteristic speed associated with a strong shock, measured relative to the grid, vanished. Since the dissipation introduced by Godunov's method vanished as the shock speed went to zero, they argued that dissipation in a slowly moving shock using Godunov's method was not sufficient to guarantee correct entropy production across the shock.

They showed an example for an extremely strong shock moving slowly from right to left. There were substantial oscillations in both the entropy and the Riemann invariant $u - 2a/(\gamma - 1)$, but the quantity $u + 2a/(\gamma - 1)$ the Riemann invariant transported along the $(u + a)$ characteristic was well behaved, where u, a, and γ are the velocity, sound speed, and ratio of specific heats, respectively. Their explanation was that in a $(u + a)$ wave any errors generated in the associated Riemann variable were immediately driven back to the shock transition layer while in the u and $u - a$ waves the errors were carried away from the shock (see Fig. 1), therefore postshock oscillations only appeared in nonlinear system of equations. Extra dissipation was added to suppress the oscillations.

More recently Roberts [3] compared Godunov's [7], Roe's, and Osher's [8] schemes on a Mach-3 shock which took 50

0021-9991/95 $6.00

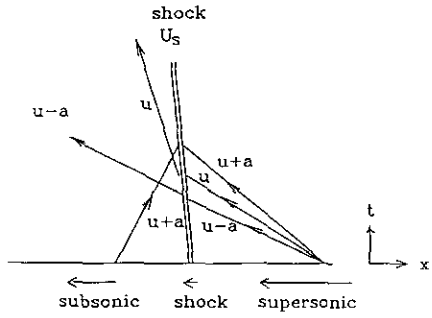

FIG. 1. Wave diagram for explaining the noise propagation.

steps to cross a cell for CFL number 0.95. He showed Osher's scheme behaved quite well while Godunov's and Roe's schemes exhibited obvious postshock oscillations not only for extremely strong shocks but also for weak shocks. He also showed that the results from Roe's scheme with minmod limiter were worse than those from the first-order Roe's scheme. The reason is because a second-order scheme has less dissipation to suppress the oscillations. One more interesting result, obtained from Osher's scheme with natural ordering of wave paths, showed that it was not as good as the original scheme which used reversed ordering of wave paths. He also argued the oscillations would occur for any schemes with flux functions that give "exact" shock resolution such as Godunov's and Roe's schemes.

2.2. *Numerical Experiments on Roe's Scheme*

Our purpose in doing the numerical experiments is to find the parameters associated with the postshock phenomena.

The initial data in our tests are obtained by superimposing a velocity on a zero-velocity shock. This velocity can be either positive or negative. The shock condition is labeled by "Mach Number X." Here the "Mach number X" shock means the shock data, such as the pressure jump, are obtained from the steady normal shock relations for Mach number X and ratio of specific heats $\gamma = 1.4$.

From numerical experiments we found the relative shock speed is important. If the shock moves slowly or fast enough then the oscillations are very small. The maximum amplitude of density oscillations for shocks moving from low density to high density region is bigger than that for shocks moving in the opposite direction, but for entropy oscillations the situation reverses. To nondimensionalise the shock velocity the shock speed is divided by the value of $(u + a)$ in the right side state. The nondimensionalised shock speed is called SR. The reason to use $(u + a)$ of right state instead of the associated characteristic speed is simply to avoid the SR value becoming too small; nevertheless, it seems to work well. Figure 2 gives the maximum amplitude of density oscillation versus SR. The SR value which produces maximum oscillation is around ± 0.035; $SR = -0.035$ with the CFL number 0.95 is very close to Roberts' test. The peak error for a downstream moving shock is higher than that of an upwind moving shock in Fig. 2. If the SR is plotted with respect to the entropy error the peak of the upstream moving shock will be bigger.

2.3. *Roe's Scheme with Dissipation*

Although Osher's Riemann solver is superior for slowly moving shock calculations, it is quite expensive computationally and difficult to use on more complicated problems, such as real gas, reacting gas, etc. because of the evaluation of the flux integral. Besides the superiority could be lost when it is used on more complicated problems where the flux integration can not be exactly evaluated.

In contrast Roe's scheme is much cheaper to run and much easier to extend to more general flow problems. Therefore we want to modify Roe's scheme to cure its postshock oscillations. We first tried to incorporate a contribution from the sonic point within a shock, which hopefully simulates Osher's Riemann solver to some extent. The results are rather disappointing. The theoretical analysis of discrete shock profile for the scalar case was made by Jennings [10]. To perform similar analysis for system is nevertheless difficult. We therefore resort to adding dissipation.

Consider the one-dimensional Euler equation

$$\frac{\partial \mathbf{W}}{\partial t} + \frac{\partial \mathbf{F}}{\partial \mathbf{W}} = 0, \tag{1}$$

where

$$\mathbf{W} = \begin{vmatrix} \rho \\ \rho u \\ e \end{vmatrix}, \quad \mathbf{F} = \begin{vmatrix} \rho u \\ \rho u^2 + P \\ u(e + P) \end{vmatrix}$$

and

$$P = (\gamma - 1)(e - 0.5\rho u^2),$$

where ρ, P, and e are the density, pressure, and energy, respectively. A first-order conservative scheme using interface flux formulation is

$$\mathbf{W}_i^{n+1} - \mathbf{W}_i^n + \frac{\Delta t}{\Delta x}[\mathbf{H}_{i+1/2}(\mathbf{W}_i^n, \mathbf{W}_{i+1}^n) - \mathbf{H}_{i-1/2}(\mathbf{W}_{i-1}^n, \mathbf{W}_i^n)] = 0, \tag{2}$$

where n is the time index and i is the grid index.

In Roe's approach, the interface flux is

$$\mathbf{H}^{\text{Roe}}(\mathbf{W}_L, \mathbf{W}_R) = \tfrac{1}{2}(\mathbf{F}_L + \mathbf{F}_R) - \tfrac{1}{2}\sum_k |\lambda_k| \alpha_k \mathbf{E}_k = 0, \tag{3}$$

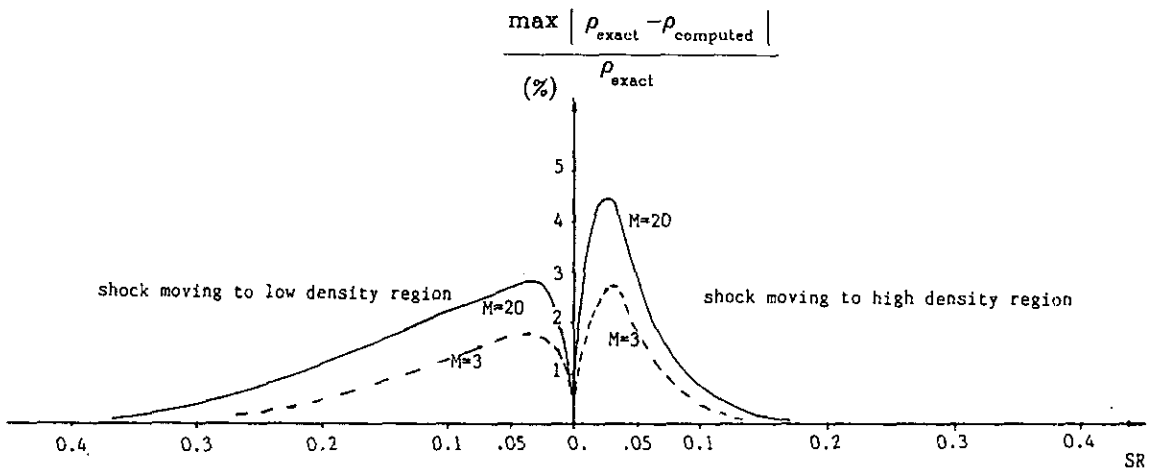

FIG. 2. Density oscillation magnitude vs *SR* for Roe's scheme.

where λ_k, α_k, and $\mathbf{E}_k$ are the eigenvalues (wave speeds), wave strengths, and eigenvectors, respectively. The wave speeds are

$$\lambda_1 = u - a, \quad \lambda_2 = u, \quad \lambda_3 = u + a \tag{4}$$

and the wave strengths and eigenvectors are given in [5].

In order to break up the unphysical solutions that can arise from this formula, Harten [11] used

$$\mathbf{H}^{\text{Harten}}(\mathbf{W}_L, \mathbf{W}_R) = \tfrac{1}{2}(\mathbf{F}_L + \mathbf{F}_R) - \tfrac{1}{2}\sum_k |Q_k|\alpha_k \mathbf{E}_k = 0, \tag{5}$$

where

$$Q_k = \begin{cases} |\nu_k|: & |\nu_k| > \delta \\ \dfrac{1}{2}\left(\dfrac{\nu_k^2 + \delta^2}{\delta}\right): & |\nu_k| \le \delta \end{cases}$$

and

$$\nu_k = \lambda_k \frac{\Delta t}{\Delta x}$$

at the expense of some deterioration in accuracy, especially at the shock.

The postshock oscillations can be suppressed by this dissipation with well-tuned δ and the solution quality can match that from Osher's scheme. But the main disadvantages are that δ needs to be adjusted for each case and it is CFL number dependent. We modify this formula by considering Q_k as a function of ν_k, $\Delta\nu_k$, and $\Delta t^{\max}$, where Q_k is the difference of the CFL number in the same type of wave and $\Delta t^{\max}$ is the local maximum allowed time steps. The modified Q_k is given by

$$Q_k = \begin{cases} |\nu_k|: & |\nu_k| > \delta \\ \dfrac{1}{2}\left(\dfrac{\nu_k^2 + \delta_k^2}{\delta_k}\right): & |\nu_k| \le \delta \end{cases} \tag{6}$$

and

$$\delta_k = \frac{\Delta t}{\Delta t^{\max}} \Delta\nu_k \delta',$$

where

$$\Delta\nu_k = |(\nu_k)_R - (\nu_k)_L|$$

and δ' is taken as 0.5 from numerical experiments. This is only implemented in the intervals which contain sonic points. Figure 3 shows side by side comparison of several schemes on the Mach 3 shock. Acceptable results are obtained with the modified dissipation.

2.4. *Second-Order TVD Schemes*

For applications, a second-order TVD scheme is usually needed. But it produces significant larger oscillations than the first-order schemes whether the Osher's or Roe's Riemann solver is adopted, see Fig. 4.

The cure we propose is that if the grid interval between left and right states contains any sonic point then we switch off the limiter. Therefore the first-order flux is used in such interface. This proves to work well. The width of shock transition does not increase and the postshock oscillations are decreased to nearly the same level of those from first-order schemes. The method is especially easy to implement in schemes using the Osher's solver, which has a built-in sonic point check. Note that in the sonic interval the limiter function is not necessarily

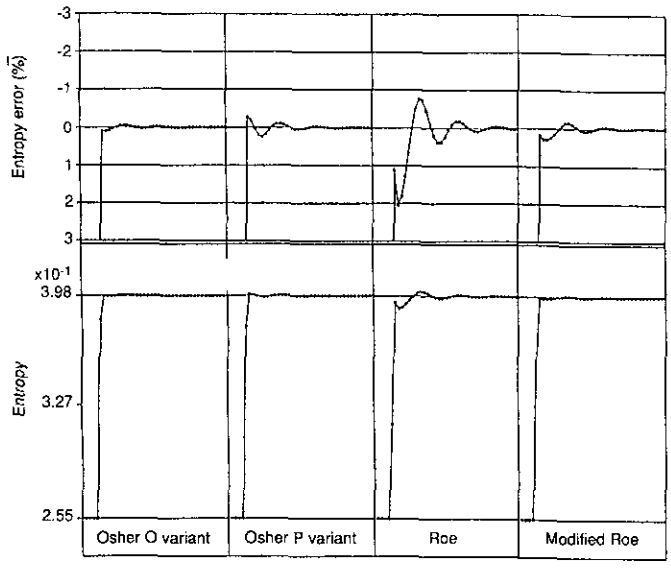

FIG. 3. Comparison of entropy oscillations for first order schemes with Mach number 3 and $SR -0.035$.

zero because inside the shock transition layer the flow may be smooth. It is only in the corner of the shock profile one can be sure that it reduces to first-order accuracy.

In general sonic points include not only the sonic point in the compression wave but also the sonic point in the expansion wave. It is well known that the numerical sonic flux for the expansion wave is not appropriate to simulate the physical expansion. Using a limiter for the sonic flux will produce worse results. Therefore it is reasonable to switch off the limiter when evaluating the sonic flux in all cases. For the second-order scheme using Roe's Riemann solver the same technique can be applied together with the dissipation described in Section 2.3. The result is much improved. Figure 4 give comparisons of results from using this approach.

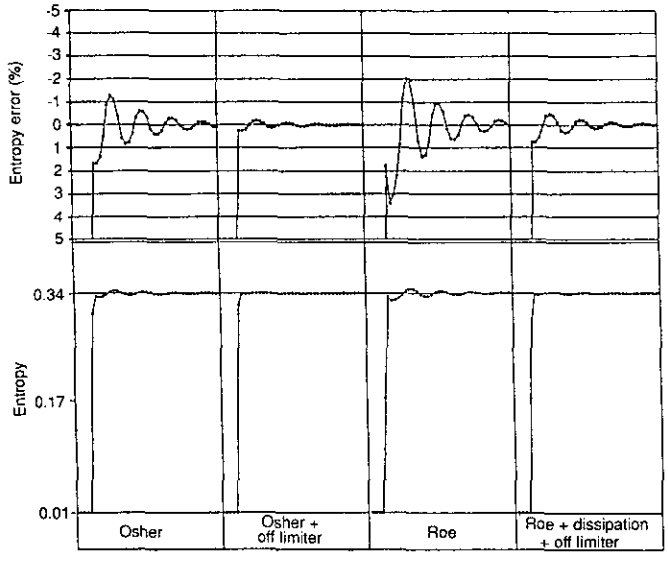

FIG. 4. Comparison of entropy oscillations for second order schemes with Mach number 20 and $SR -0.035$ (Lax–Wendroff TVD scheme with minmod limiter).

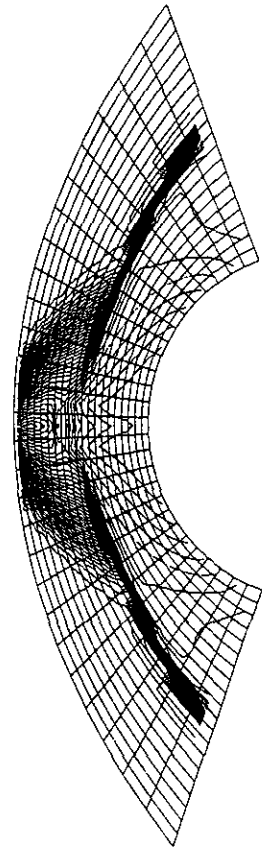

FIG. 5. A typical carbuncle phenomenon at Mach number 8 using first-order Roe/Osher scheme.

This method should be quite useful for the unsteady calculations; however, it is found that this limiter-off approach is not suitable for implicit schemes for steady state calculations because it introduces nonsmoothness, which usually cause convergence difficulties.

3. THE CARBUNCLE PHENOMENON

3.1. *Introduction*

It has been observed by some people for some time that Roe's and Osher's approximate Riemann solvers produce instability when used to compute supersonic flow over blunt bodies, e.g., Fig. 5. Nevertheless it is only recently that Peery and Imlay [4] first reported this instability in the literature. According to them this instability was called the "carbuncle phenomenon" by the researchers at NASA. The reason for such behaviour is not clear.

If one uses the free stream condition as an initial condition, the bow shock will form at the solid boundary then gradually travel to its final position. During the early shock evolution there is no problem. It is when the shock approaches its final position that the instability begins to appear. Sometimes the solution breaks down completely. In some cases the instability phenomenon is not obvious and the shape of the bow shock looks fairly normal but one can still see from the Mach contour plot that the constant Mach lines are not circular but distorted inside the subsonic pocket.

Peery and Imlay also reported the flux vector splitting of Steger and Warming [12] had no such problem. Together with our own experience on the flux vector splitting of Van Leer [13] the flux vector splitting schemes appear to be clear of the carbuncle phenomenon, although they do have other problems (see Section 3.2).

In the two-dimensional problem the flux difference schemes solve the Riemann problem normal to the grid boundary, e.g., Chakravarthy and Osher [14]. In two dimensions there are four waves,

$$\lambda_1 = V_n - a, \quad \lambda_{2,3} = V_n, \quad \lambda_4 = V_n + a, \tag{7}$$

where V_n and a are the normal velocity with respect to the grid interface and the interface sound speed, respectively. When Roe's Riemann solver is used, the formula due to Yee [6] is the most popular to aid convergence and to break possible unphysical expansion shocks. In Yee's formula the $Q(\lambda_k)$, which replaces λ_k, is given by

$$Q_k = \begin{cases} |\lambda_k|: & |\lambda_k| > \delta_k \\ \dfrac{1}{2}\left[\operatorname{sign}(\lambda_k)\dfrac{\lambda_k^2 + \delta_k^2}{\delta_k} + \lambda_k\right]: & |\lambda_k| \le \delta_k, \end{cases} \tag{8}$$

where

$$\delta_k = \delta_k^*(|V_n| + |V_t| + a). \tag{9}$$

Here V_t is the tangential velocity with respect to the grid interface. Note that a more appropriate extension of Harten's dissipation in Section 2.3 is to use

$$\delta_k = \delta_k^*(|V_n| + a). \tag{10}$$

The dissipation is not necessary for V_n waves for breaking expansion shocks; however, in the supersonic blunt body calculation we do need it for the V_n waves. for the second-order upwind TVD scheme we used (see [9] for more details) the dissipation coefficients for V_n linear waves have to be set to quite a large value to overcome this instability but the coefficients for $V_n + a$ and $V_n - a$ waves are not important. The necessity to add dissipation on the V_n waves might explain why the flux-vector splitting does not have this problem since it is very dissipative for the V_n waves.

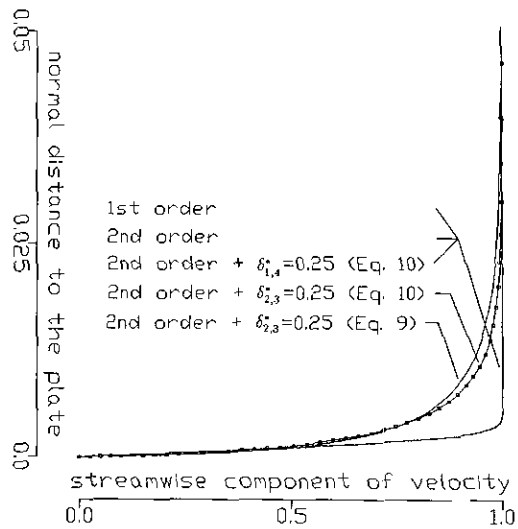

FIG. 6. Dissipation effect on numerical boundary layer thickness.

We need a larger number for δ_2^* and δ_3^* than that for the symmetric TVD scheme of Yee. Nevertheless Pfitzner *et al.* [15] reported that even for the first-order scheme the values of δ_k^* have to be greater than 0.25, which agrees with our experiences, although 0.25 seemed to be the largest value Yee [6] employed.

3.2. *Dissipation Effect on Numerical Boundary Layer Thickness*

It is well known that Roe's Riemann solver, which includes information about all waves, can give very accurate representation of boundary layers in quite a coarse mesh while Van Leer's flux-vector splitting, which ignores the linear waves, badly diffuses the boundary layer (Van Leer *et al.* [16]). Thus, any formulas which add dissipation to the linear waves, e.g., Yee's, degrade the solution for viscous calculations.

An easy demonstration is to check the numerical boundary layer thickness on a flat plate. A numerical scheme with more dissipation will give a thicker numerical boundary layer. The test uses free stream Mach number 0.8 and the adiabatic wall condition. Along the streamwise direction there are 10 cells before the leading edge and 40 cells along the plate with uniform mesh spacing. There are 50 cells in the direction normal to the plate. The largest gird aspect ration is 1000. Figure 6 shows the velocity profiles at the last column cells normal to the plate, where the Re_x is 1,997,500. The first-order and second-order schemes without any dissipation and with $\delta_{1,4}^* = 0.25$ (Eq. 10) give nearly the same results. With $\delta_{2,3}^* = 0.25$ (Eq. 9) or (Eq. 10) the calculated boundary layer thickness is unacceptably large. We therefore do not recommend Yee's dissipation for viscous calculations and any proposed method for curing the blunt nose instability should pass this test case also.

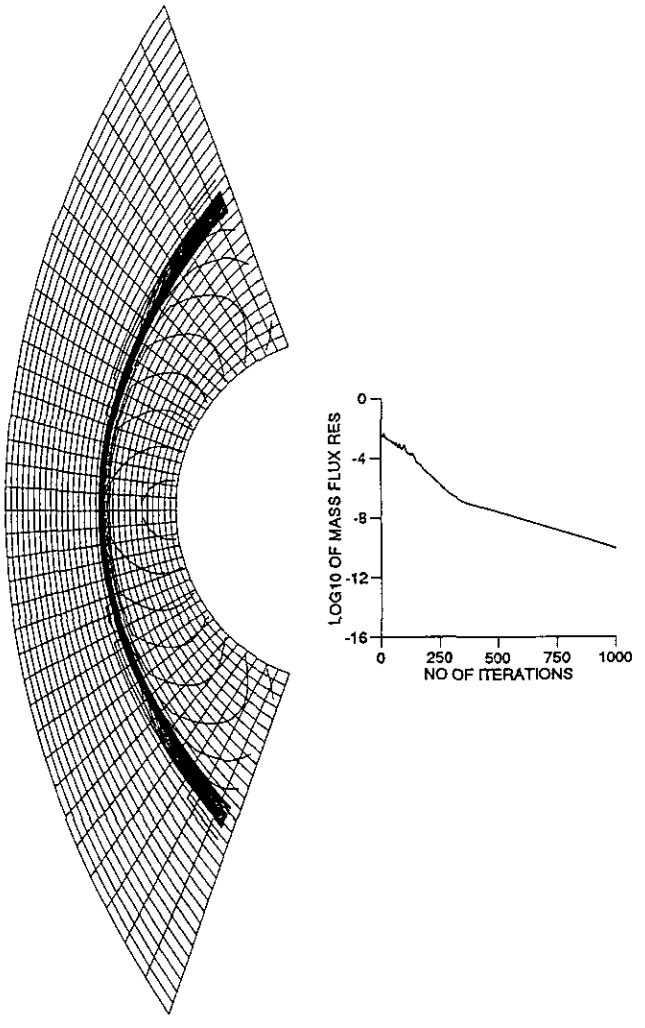

FIG. 7. Mach contour and convergence history for Mach number 8 flow with $k_1 = 0.25$, $k_2 = 0$, and $k_3 = 15$.

Von Lavante [17] also made similar investigation on comparing the resolution of boundary layer by Roe's Riemann solver and Van Leer's flux-vector splitting schemes. His result also showed that Yee's formula degrades the solution significantly.

3.3. *Formula of Peery and Imlay and Its Improvement*

The drawback of Yee's formula was also understood by Peery and Imlay [4]. They proposed a formula which uses the pressure gradient to tune the magnitude of the dissipation. They changed the eigenvalues (wave speeds) to

$$\lambda_k' = \frac{1}{2}\left(\frac{\lambda_k^2 + \varepsilon_k^2}{\varepsilon_k}\right), \tag{11}$$

where

$$\varepsilon_{1,4} = \begin{cases} 1.2(|V_n + a) + \dfrac{\Delta^2 P}{4P^*} V_\infty: & \text{in } i \text{ direction} \\ 0.2(|V_n + a) + \dfrac{\Delta^2 P}{4P^*} V_\infty: & \text{in } j \text{ direction} \end{cases}$$

$$\varepsilon_{2,3} = \begin{cases} (|V_n + a) + \dfrac{\Delta^2 P}{4P^*} V_\infty: & \text{in } i \text{ direction} \\ \dfrac{\Delta^2 P}{4P^*} V_\infty: & \text{in } j \text{ direction.} \end{cases}$$

In their words, $\Delta^2 P$ is a second difference of pressure averaged at the cell face, P^* is an averaged local pressure, and V_∞ is the free stream total velocity. They solved for a Mach 2 flow past

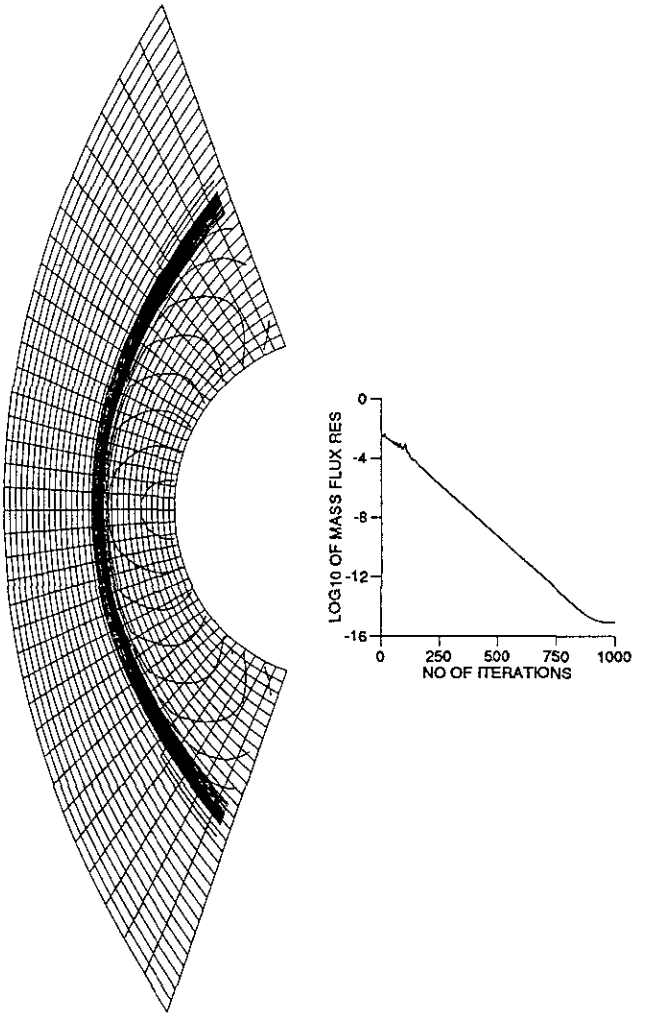

FIG. 8. Mach contour and convergence history for Mach number 8 flow with $k_1 = 0.25$, $k_2 = 5$, and $k_3 = 15$.

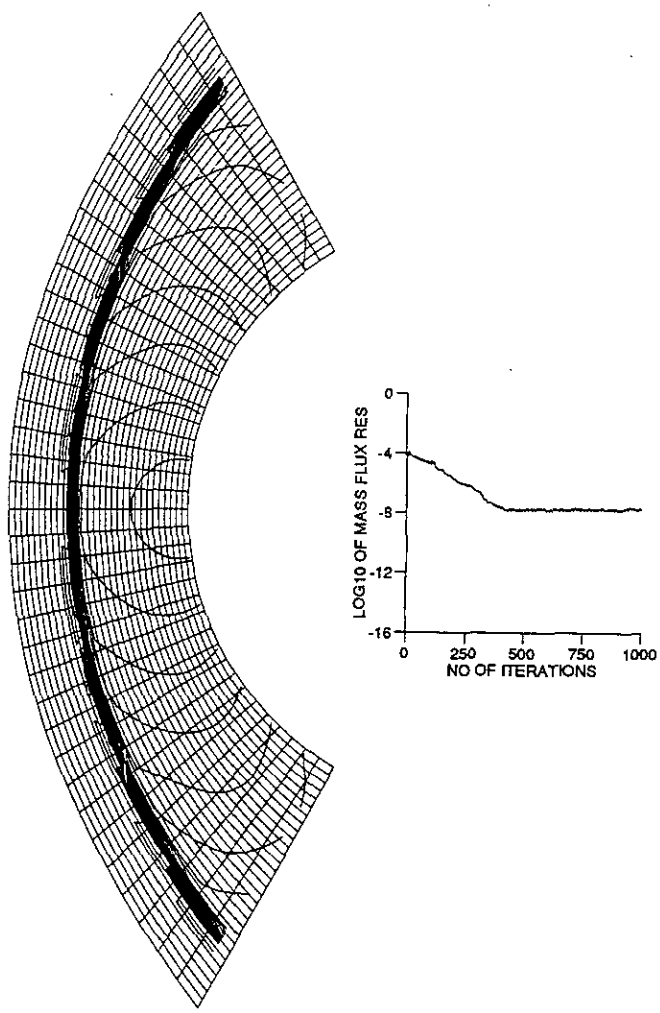

FIG. 9. Mach contour and convergence history for Mach number 20 flow with $k_1 = 0.25$, $k_2 = 0$, and $k_3 = 15$.

a flat plate, to demonstrate their formula is suitable for viscous calculation when the j direction is normal to the wall. Nevertheless, their formula is still not suitable for viscous blunt-body calculation if the i direction, which was bigger dissipation, is normal to the body or when it is used to compute the flow with an angle of attack. Another problem of their formula is that, again in their words, the shock was captured with approximately three internal points, although the outer two points were nearly equal to the conditions at the edges of the shock. This is due to the excessive dissipation at the supersonic part of flow.

Their idea of using the pressure gradient to tune the dissipation seems to be a good idea. We still use Eq. (8) in Section 3.1 but we change the δ_k. Our modification is

$$\begin{aligned} \delta_{1,4} &= (|V_n| + a)(k_1 + k_2 k_p) \\ \delta_{2,3} &= (|V_n| + a)(k_3 k_p); \end{aligned} \tag{12}$$

k_p is similar to $\Delta^2 P$, k_1 serves as the basic dissipation to break unphysical expansion shock, k_2 is for smoothing the staircase shock profile, and k_3 is to prevent the instability. The k_p at interface $(i + \frac{1}{2}, j)$, for example, is equal to the average of k_p at $(i + 1, j)$ and (i, j). The k_p at (i, j) is chosen as a formula similar to that introduced by Jameson *et al.*[18] for stabilising central-difference shock calculations. It is given as

$$(k_p)_{i,j} = 0.5 \left(\left| \frac{P_{i+1,j} - 2P_{i,j} + P_{i-1,j}}{P_{i+1,j} + 2P_{i,j} + P_{i-1,j}} \right| + \left| \frac{P_{i,j+1} - 2P_{i,j} + P_{i,j-1}}{P_{i,j+1} + 2P_{i,j} + P_{i,j-1}} \right| \right) \tag{13}$$

and if the local Mach number at cell (i, j) is greater than 1.0 then k_p is divided by the local Mach number to decrease the dissipation in the supersonic region. The reason to average the pressure at two different directions is because large dissipation

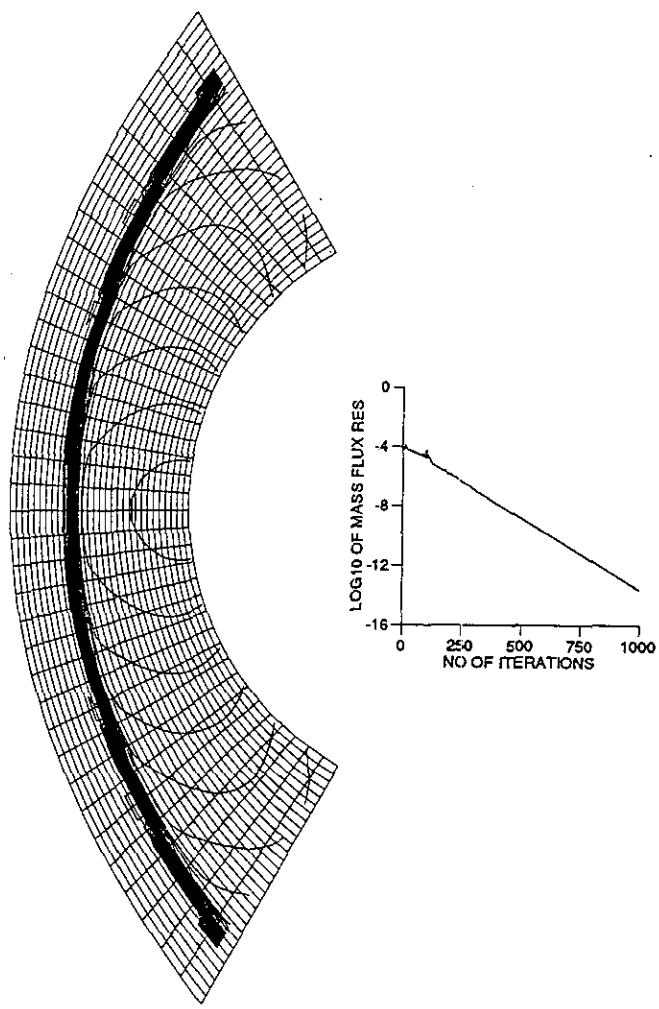

FIG. 10. Mach contour and convergence history for Mach number 20 flow with $k_1 = 0.25$, $k_2 = 5$, and $k_3 = 15$.

parallel to the shock is found necessary to cure instability and, using the pressure gradient parallel to the shock alone, it will be too small to maintain stability. Also, the averaging process to define the k_p at the cell interface smooths dissipation and thus helps convergence when implicit schemes are used.

Our modification removes the directional dependency of Peery and Imlay's formula and decreases the dissipation in supersonic regions, thus it sharpens the shock transition profile. For this formula the magnitude of k_p is about the order of 10^{-3} to 10^{-4} in smooth flow and so the total numerical damping is very small for the linear waves. There are at most two internal points in the shock transition layer with our formula. Figure 7 shows the result for Mach 8 calculation with $k_1 = 0.25$, $k_2 = 0$, and $k_3 = 15$. Figure 8 is obtained with $k_2 = 5$. Figures 9 and 10 show the results for Mach 20 using the same parameters as Figs. 7 and 8, respectively. From these graphs the solutions converge better with $k_2 = 5$, which helps to smooth the staircase-like bow shock profile. The implicit scheme used is a conservative DDADI scheme; see [9] for more details.

4. CONCLUSION

In this paper we have demonstrated a cure for Roe's Riemann solver on the slowly moving shock problem based on the difference of associated wave speeds, a limiter-off approach for any higher order schemes, and an improved formula to prevent the carbuncle phenomenon, especially for viscous flow calculations.

In general more information about the slowly moving shock problem and carbuncle phenomenon are revealed, although the reasons for the superiority of Osher's Riemann solver on the slowly moving shock problem and the carbuncle phenomenon of flux-difference splitting remain unknown. More study is certainly needed.

ACKNOWLEDGMENTS

The author thanks Professor P. L. Roe for many of his suggestions and the reviewers for their comments and suggestions.

REFERENCES

1. P. L. Roe, *in* "11th Int. Conf. on Num. Meth. in Fluid Dyn.," Lectures Notes in Physics (Springer-Verlag, Berlin, 1988).
2. P. Colella and P. R. Woodward, *J. Comput. Phys.* **54,** 174 (1984).
3. T. W. Roberts, in *Numerical Methods for Fluid Dynamics III,* edited by K. W. Morton and M. J. Baines (Clarendon Press, Oxford, 1988).
4. K. M. Peery and S. T. Imlay, AIAA Paper 88-2904, 1988 (unpublished).
5. P. L. Roe, *J. Comput. Phys.* **43,** 357 (1981).
6. H. C. Yee, NASA TM89464, 1987 (unpublished).
7. S. K. Godunov, *Math. Sb.* **47,** 217 (1959).
8. S. Osher and F. Soloman, *Math. Comput.* **18,** 339 (1982).
9. H. Lin, Ph.D. thesis, College of Aeronautics, Cranfield Institute of Technology, 1990.
10. G. Jennings, *Commun. Pure Appl. Math.* **27,** 25 (1974).
11. A. Harten, *J. Comput. Phys.* **49,** 357 (1983).
12. J. L. Steger and R. F. Warming, *J. Comput. Phys.* **40,** 395 (1981).
13. B. Van Leer, Lect. Notes in Phys., Vol. 170, pp. 507, (Springer-Verlag, New York/Berlin, 1982).
14. S. R. Chakravarthy and S. Osher, AIAA Paper 85-0363, 1985 (unpublished).
15. M. Pfitzner, W. Schroeder, S. Menne, and C. Weiland, *in* "Proceedings, Int. Conf. on Hypersonic Aerodynamics, Royal Aeronautical Society, 1989."
16. B. Van Leer *et al.,* AIAA Paper 87-1104, 1987 (unpublished).
17. E. Von Lavante, *AIAA J.* **28,** 1312 (1990).
18. A. Jameson, W. Schmidt, and E. Turkel, AIAA Paper 81-1259, 1981 (unpublished).